ISSN 1726-5749

SENSORS & TRANSDUCERS

vol. 5
Special
3/09

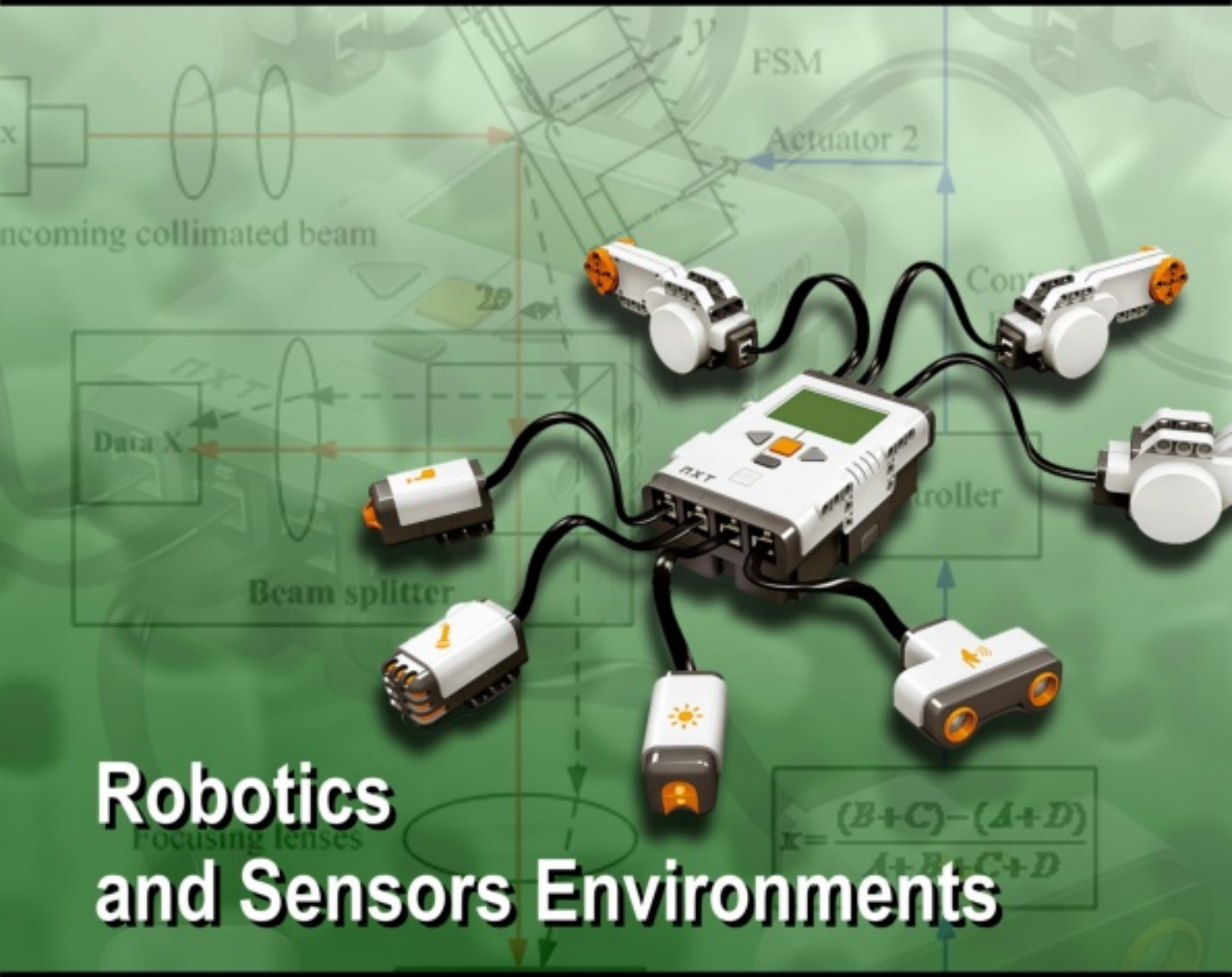

Robotics and Sensors Environments

International Frequency Sensor Association Publishing

IFSA

Sensors & Transducers

Volume 4, Special Issue
March 2009

www.sensorsportal.com

ISSN 1726-5479

Guest Editors: Dr. Pierre Payeur and Dr. Emil M. Petriu, University of Ottawa, Ottawa, ON, Canada
Editor-in-Chief: professor Sergey Y. Yurish, phone: +34 696067716, fax: +34 93 4011989, e-mail: editor@sensorsportal.com

Editors for Western Europe
Meijer, Gerard C.M., Delft University of Technology, The Netherlands
Ferrari, Vittorio, Universitá di Brescia, Italy

Editor South America
Costa-Felix, Rodrigo, Inmetro, Brazil

Editor for Eastern Europe
Sachenko, Anatoly, Ternopil State Economic University, Ukraine

Editors for North America
Datskos, Panos G., Oak Ridge National Laboratory, USA
Fabien, J. Josse, Marquette University, USA
Katz, Evgeny, Clarkson University, USA

Editor for Asia
Ohyama, Shinji, Tokyo Institute of Technology, Japan

Editor for Asia-Pacific
Mukhopadhyay, Subhas, Massey University, New Zealand

Editorial Advisory Board

Abdul Rahim, Ruzairi, Universiti Teknologi, Malaysia
Ahmad, Mohd Noor, Nothern University of Engineering, Malaysia
Annamalai, Karthigeyan, National Institute of Advanced Industrial Science and Technology, Japan
Arcega, Francisco, University of Zaragoza, Spain
Arguel, Philippe, CNRS, France
Ahn, Jae-Pyoung, Korea Institute of Science and Technology, Korea
Arndt, Michael, Robert Bosch GmbH, Germany
Ascoli, Giorgio, George Mason University, USA
Atalay, Selcuk, Inonu University, Turkey
Atghiaee, Ahmad, University of Tehran, Iran
Augutis, Vygantas, Kaunas University of Technology, Lithuania
Avachit, Patil Lalchand, North Maharashtra University, India
Ayesh, Aladdin, De Montfort University, UK
Bahreyni, Behraad, University of Manitoba, Canada
Baoxian, Ye, Zhengzhou University, China
Barford, Lee, Agilent Laboratories, USA
Barlingay, Ravindra, RF Arrays Systems, India
Basu, Sukumar, Jadavpur University, India
Beck, Stephen, University of Sheffield, UK
Ben Bouzid, Sihem, Institut National de Recherche Scientifique, Tunisia
Benachaiba, Chellali, Universitaire de Bechar, Algeria
Binnie, T. David, Napier University, UK
Bischoff, Gerlinde, Inst. Analytical Chemistry, Germany
Bodas, Dhananjay, IMTEK, Germany
Borges Carval, Nuno, Universidade de Aveiro, Portugal
Bousbia-Salah, Mounir, University of Annaba, Algeria
Bouvet, Marcel, CNRS – UPMC, France
Brudzewski, Kazimierz, Warsaw University of Technology, Poland
Cai, Chenxin, Nanjing Normal University, China
Cai, Qingyun, Hunan University, China
Campanella, Luigi, University La Sapienza, Italy
Carvalho, Vitor, Minho University, Portugal
Cecelja, Franjo, Brunel University, London, UK
Cerda Belmonte, Judith, Imperial College London, UK
Chakrabarty, Chandan Kumar, Universiti Tenaga Nasional, Malaysia
Chakravorty, Dipankar, Association for the Cultivation of Science, India
Changhai, Ru, Harbin Engineering University, China
Chaudhari, Gajanan, Shri Shivaji Science College, India
Chen, Jiming, Zhejiang University, China
Chen, Rongshun, National Tsing Hua University, Taiwan
Cheng, Kuo-Sheng, National Cheng Kung University, Taiwan
Chiang, Jeffrey (Cheng-Ta), Industrial Technol. Research Institute, Taiwan
Chiriac, Horia, National Institute of Research and Development, Romania
Chowdhuri, Arijit, University of Delhi, India
Chung, Wen-Yaw, Chung Yuan Christian University, Taiwan
Corres, Jesus, Universidad Publica de Navarra, Spain
Cortes, Camilo A., Universidad Nacional de Colombia, Colombia
Courtois, Christian, Universite de Valenciennes, France
Cusano, Andrea, University of Sannio, Italy
D'Amico, Arnaldo, Università di Tor Vergata, Italy
De Stefano, Luca, Institute for Microelectronics and Microsystem, Italy
Deshmukh, Kiran, Shri Shivaji Mahavidyalaya, Barshi, India
Dickert, Franz L., Vienna University, Austria
Dieguez, Angel, University of Barcelona, Spain
Dimitropoulos, Panos, University of Thessaly, Greece
Ding Jian, Ning, Jiangsu University, China
Djordjevich, Alexandar, City University of Hong Kong, Hong Kong
Donato, Nicola, University of Messina, Italy
Donato, Patricio, Universidad de Mar del Plata, Argentina
Dong, Feng, Tianjin University, China
Drljaca, Predrag, Instersema Sensoric SA, Switzerland
Dubey, Venketesh, Bournemouth University, UK
Enderle, Stefan, University of Ulm and KTB Mechatronics GmbH, Germany
Erdem, Gursan K. Arzum, Ege University, Turkey
Erkmen, Aydan M., Middle East Technical University, Turkey
Estelle, Patrice, Insa Rennes, France
Estrada, Horacio, University of North Carolina, USA
Faiz, Adil, INSA Lyon, France
Fericean, Sorin, Balluff GmbH, Germany
Fernandes, Joana M., University of Porto, Portugal
Francioso, Luca, CNR-IMM Institute for Microelectronics and Microsystems, Italy
Francis, Laurent, University Catholique de Louvain, Belgium
Fu, Weiling, South-Western Hospital, Chongqing, China
Gaura, Elena, Coventry University, UK
Geng, Yanfeng, China University of Petroleum, China
Gole, James, Georgia Institute of Technology, USA
Gong, Hao, National University of Singapore, Singapore
Gonzalez de la Rosa, Juan Jose, University of Cadiz, Spain
Granel, Annette, Goteborg University, Sweden
Graff, Mason, The University of Texas at Arlington, USA
Guan, Shan, Eastman Kodak, USA
Guillet, Bruno, University of Caen, France
Guo, Zhen, New Jersey Institute of Technology, USA
Gupta, Narendra Kumar, Napier University, UK
Hadjiloucas, Sillas, The University of Reading, UK
Hashsham, Syed, Michigan State University, USA
Hernandez, Alvaro, University of Alcala, Spain
Hernandez, Wilmar, Universidad Politecnica de Madrid, Spain
Homentcovschi, Dorel, SUNY Binghamton, USA
Horstman, Tom, U.S. Automation Group, LLC, USA
Hsiai, Tzung (John), University of Southern California, USA
Huang, Jeng-Sheng, Chung Yuan Christian University, Taiwan
Huang, Star, National Tsing Hua University, Taiwan
Huang, Wei, PSG Design Center, USA
Hui, David, University of New Orleans, USA
Jaffrezic-Renault, Nicole, Ecole Centrale de Lyon, France
Jaime Calvo-Galleg, Jaime, Universidad de Salamanca, Spain
James, Daniel, Griffith University, Australia
Janting, Jakob, DELTA Danish Electronics, Denmark
Jiang, Liudi, University of Southampton, UK
Jiang, Wei, University of Virginia, USA
Jiao, Zheng, Shanghai University, China
John, Joachim, IMEC, Belgium
Kalach, Andrew, Voronezh Institute of Ministry of Interior, Russia
Kang, Moonho, Sunmoon University, Korea South
Kaniusas, Eugenijus, Vienna University of Technology, Austria
Katake, Anup, Texas A&M University, USA
Kausel, Wilfried, University of Music, Vienna, Austria
Kavasoglu, Nese, Mugla University, Turkey
Ke, Cathy, Tyndall National Institute, Ireland
Khan, Asif, Aligarh Muslim University, Aligarh, India
Kim, Min Young, Kyungpook National University, Korea South
Sandacci, Serghei, Sensor Technology Ltd., UK

Ko, Sang Choon, Electronics and Telecommunications Research Institute, Korea South
Kockar, Hakan, Balikesir University, Turkey
Kotulska, Malgorzata, Wroclaw University of Technology, Poland
Kratz, Henrik, Uppsala University, Sweden
Kumar, Arun, University of South Florida, USA
Kumar, Subodh, National Physical Laboratory, India
Kung, Chih-Hsien, Chang-Jung Christian University, Taiwan
Lacnjevac, Caslav, University of Belgrade, Serbia
Lay-Ekuakille, Aime, University of Lecce, Italy
Lee, Jang Myung, Pusan National University, Korea South
Lee, Jun Su, Amkor Technology, Inc. South Korea
Lei, Hua, National Starch and Chemical Company, USA
Li, Genxi, Nanjing University, China
Li, Hui, Shanghai Jiaotong University, China
Li, Xian-Fang, Central South University, China
Liang, Yuanchang, University of Washington, USA
Liawruangrath, Saisunee, Chiang Mai University, Thailand
Liew, Kim Meow, City University of Hong Kong, Hong Kong
Lin, Hermann, National Kaohsiung University, Taiwan
Lin, Paul, Cleveland State University, USA
Linderholm, Pontus, EPFL - Microsystems Laboratory, Switzerland
Liu, Aihua, University of Oklahoma, USA
Liu Changgeng, Louisiana State University, USA
Liu, Cheng-Hsien, National Tsing Hua University, Taiwan
Liu, Songqin, Southeast University, China
Lodeiro, Carlos, Universidade NOVA de Lisboa, Portugal
Lorenzo, Maria Encarnacio, Universidad Autonoma de Madrid, Spain
Lukaszewicz, Jerzy Pawel, Nicholas Copernicus University, Poland
Ma, Zhanfang, Northeast Normal University, China
Majstorovic, Vidosav, University of Belgrade, Serbia
Marquez, Alfredo, Centro de Investigacion en Materiales Avanzados, Mexico
Matay, Ladislav, Slovak Academy of Sciences, Slovakia
Mathur, Prafull, National Physical Laboratory, India
Maurya, D.K., Institute of Materials Research and Engineering, Singapore
Mekid, Samir, University of Manchester, UK
Melnyk, Ivan, Photon Control Inc., Canada
Mendes, Paulo, University of Minho, Portugal
Mennell, Julie, Northumbria University, UK
Mi, Bin, Boston Scientific Corporation, USA
Minas, Graca, University of Minho, Portugal
Moghavvemi, Mahmoud, University of Malaya, Malaysia
Mohammadi, Mohammad-Reza, University of Cambridge, UK
Molina Flores, Esteban, Benemérita Universidad Autónoma de Puebla, Mexico
Moradi, Majid, University of Kerman, Iran
Morello, Rosario, DIMET, University "Mediterranea" of Reggio Calabria, Italy
Mounir, Ben Ali, University of Sousse, Tunisia
Mulla, Imtiaz Sirajuddin, National Chemical Laboratory, Pune, India
Neelamegam, Periasamy, Sastra Deemed University, India
Neshkova, Milka, Bulgarian Academy of Sciences, Bulgaria
Oberhammer, Joachim, Royal Institute of Technology, Sweden
Ould Lahoucine, Cherif, University of Guelma, Algeria
Pamidighanta, Sayanu, Bharat Electronics Limited (BEL), India
Pan, Jisheng, Institute of Materials Research & Engineering, Singapore
Park, Joon-Shik, Korea Electronics Technology Institute, Korea South
Penza, Michele, ENEA C.R., Italy
Pereira, Jose Miguel, Instituto Politecnico de Setebal, Portugal
Petsev, Dimiter, University of New Mexico, USA
Pogacnik, Lea, University of Ljubljana, Slovenia
Post, Michael, National Research Council, Canada
Prance, Robert, University of Sussex, UK
Prasad, Ambika, Gulbarga University, India
Prateepasen, Asa, Kingmoungut's University of Technology, Thailand
Pullini, Daniele, Centro Ricerche FIAT, Italy
Pumera, Martin, National Institute for Materials Science, Japan
Radhakrishnan, S. National Chemical Laboratory, Pune, India
Rajanna, K., Indian Institute of Science, India
Ramadan, Qasem, Institute of Microelectronics, Singapore
Rao, Basuthkar, Tata Inst. of Fundamental Research, India
Raoof, Kosai, Joseph Fourier University of Grenoble, France
Reig, Candid, University of Valencia, Spain
Restivo, Maria Teresa, University of Porto, Portugal
Robert, Michel, University Henri Poincare, France
Rezazadeh, Ghader, Urmia University, Iran
Royo, Santiago, Universitat Politecnica de Catalunya, Spain
Rodriguez, Angel, Universidad Politecnica de Cataluna, Spain
Rothberg, Steve, Loughborough University, UK
Sadana, Ajit, University of Mississippi, USA
Sadeghian Marnani, Hamed, TU Delft, The Netherlands
Sapozhnikova, Ksenia, D.I.Mendeleyev Institute for Metrology, Russia
Saxena, Vibha, Bhbha Atomic Research Centre, Mumbai, India
Schneider, John K., Ultra-Scan Corporation, USA
Seif, Selemani, Alabama A & M University, USA
Seifter, Achim, Los Alamos National Laboratory, USA
Sengupta, Deepak, Advance Bio-Photonics, India
Shankar, B. Baliga, General Monitors Transnational, USA
Shearwood, Christopher, Nanyang Technological University, Singapore
Shin, Kyuho, Samsung Advanced Institute of Technology, Korea
Shmaliy, Yuriy, Kharkiv National University of Radio Electronics, Ukraine
Silva Girao, Pedro, Technical University of Lisbon, Portugal
Singh, V. R., National Physical Laboratory, India
Slomovitz, Daniel, UTE, Uruguay
Smith, Martin, Open University, UK
Soleymanpour, Ahmad, Damghan Basic Science University, Iran
Somani, Prakash R., Centre for Materials for Electronics Technol., India
Srinivas, Talabattula, Indian Institute of Science, Bangalore, India
Srivastava, Arvind K., Northwestern University, USA
Stefan-van Staden, Raluca-Ioana, University of Pretoria, South Africa
Sumriddetchka, Sarun, National Electronics and Computer Technology Center, Thailand
Sun, Chengliang, Polytechnic University, Hong-Kong
Sun, Dongming, Jilin University, China
Sun, Junhua, Beijing University of Aeronautics and Astronautics, China
Sun, Zhiqiang, Central South University, China
Suri, C. Raman, Institute of Microbial Technology, India
Sysoev, Victor, Saratov State Technical University, Russia
Szewczyk, Roman, Industrial Research Institute for Automation and Measurement, Poland
Tan, Ooi Kiang, Nanyang Technological University, Singapore,
Tang, Dianping, Southwest University, China
Tang, Jaw-Luen, National Chung Cheng University, Taiwan
Teker, Kasif, Frostburg State University, USA
Thumbavanam Pad, Kartik, Carnegie Mellon University, USA
Tian, Gui Yun, University of Newcastle, UK
Tsiantos, Vassilios, Technological Educational Institute of Kaval, Greece
Tsigara, Anna, National Hellenic Research Foundation, Greece
Twomey, Karen, University College Cork, Ireland
Valente, Antonio, University, Vila Real, - U.T.A.D., Portugal
Vaseashta, Ashok, Marshall University, USA
Vazquez, Carmen, Carlos III University in Madrid, Spain
Vieira, Manuela, Instituto Superior de Engenharia de Lisboa, Portugal
Vigna, Benedetto, STMicroelectronics, Italy
Vrba, Radimir, Brno University of Technology, Czech Republic
Wandelt, Barbara, Technical University of Lodz, Poland
Wang, Jiangping, Xi'an Shiyou University, China
Wang, Kedong, Beihang University, China
Wang, Liang, Advanced Micro Devices, USA
Wang, Mi, University of Leeds, UK
Wang, Shinn-Fwu, Ching Yun University, Taiwan
Wang, Wei-Chih, University of Washington, USA
Wang, Wensheng, University of Pennsylvania, USA
Watson, Steven, Center for NanoSpace Technologies Inc., USA
Weiping, Yan, Dalian University of Technology, China
Wells, Stephen, Southern Company Services, USA
Wolkenberg, Andrzej, Institute of Electron Technology, Poland
Woods, R. Clive, Louisiana State University, USA
Wu, DerHo, National Pingtung University of Science and Technology, Taiwan
Wu, Zhaoyang, Hunan University, China
Xiu Tao, Ge, Chuzhou University, China
Xu, Lisheng, The Chinese University of Hong Kong, Hong Kong
Xu, Tao, University of California, Irvine, USA
Yang, Dongfang, National Research Council, Canada
Yang, Wuqiang, The University of Manchester, UK
Ymeti, Aurel, University of Twente, Netherland
Yong Zhao, Northeastern University, China
Yu, Haihu, Wuhan University of Technology, China
Yuan, Yong, Massey University, New Zealand
Yufera Garcia, Alberto, Seville University, Spain
Zagnoni, Michele, University of Southampton, UK
Zeni, Luigi, Second University of Naples, Italy
Zhong, Haoxiang, Henan Normal University, China
Zhang, Minglong, Shanghai University, China
Zhang, Qintao, University of California at Berkeley, USA
Zhang, Weiping, Shanghai Jiao Tong University, China
Zhang, Wenming, Shanghai Jiao Tong University, China
Zhou, Zhi-Gang, Tsinghua University, China
Zorzano, Luis, Universidad de La Rioja, Spain
Zourob, Mohammed, University of Cambridge, UK

Sensors & Transducers Journal (ISSN 1726-5479) is a peer review international journal published monthly online by International Frequency Sensor Association (IFSA).
Available in electronic and CD-ROM. Copyright © 2009 by International Frequency Sensor Association. All rights reserved.

Sensors & Transducers Journal

Contents

Volume 5
Special Issue
March 2009

www.sensorsportal.com

ISSN 1726-5479

Research Articles

Foreword
Pierre Payeur and Emil Petriu 1

An Omnidirectional Stereoscopic System for Mobile Robot Navigation
Rémi Boutteau, Xavier Savatier, Jean-Yves Ertaud, Bélahcène Mazari 3

Movement in Collaborative Robotic Environments Based on the Fish Shoal Emergent Patterns
Razvan Cioarga, Mihai V. Micea, Vladimir Cretu, Emil M. Petriu..... 18

A Multiscale Calibration of a Photon Videomicroscope for Visual Servo Control: Application to MEMS Micromanipulation and Microassembly
Brahim Tamadazte, Sounkalo Dembélé and Nadine Piat..... 37

A Study on Dynamic Stiffening of a Rotating Beam with a Tip Mass
Shengjian Bai, Pinhas Ben-Tzvi, Qingkun Zhou, Xinsheng Huang..... 53

Towards a Model and Specification for Visual Programming of Massively Distributed Embedded Systems
Meng Wang, Varun Subramanian, Alex Doboli, Daniel Curiac, Dan Pescaru and Codruta Istin 69

Feature Space Dimensionality Reduction for Real-Time Vision-Based Food Inspection
Mai Moussa CHETIMA and Pierre PAYEUR 86

Design and Analysis of a Fast Steering Mirror for Precision Laser Beams Steering
Qingkun Zhou, Pinhas Ben-Tzvi and Dapeng Fan..... 104

Neural Gas and Growing Neural Gas Networks for Selective 3D Sensing: a Comparative Study
Ana-Maria Cretu, Pierre Payeur and Emil M. Petriu..... 119

Authors are encouraged to submit article in MS Word (doc) and Acrobat (pdf) formats by e-mail: editor@sensorsportal.com
Please visit journal's webpage with preparation instructions: http://www.sensorsportal.com/HTML/DIGEST/Submition.htm

Sensors & Transducers Journal, Vol. 5, Special Issue, March 2009, pp. 53-68

www.sensorsportal.com

Sensors & Transducers

ISSN 1726-5479
© 2009 by IFSA
http://www.sensorsportal.com

A Study on Dynamic Stiffening of a Rotating Beam with a Tip Mass

[1]Shengjian BAI, [2]Pinhas BEN-TZVI, [1]Qingkun ZHOU, [1]Xinsheng HUANG

[1] College of Mechatronics Engineering and Automation, National University of Defense Technology, Changsha Hunan 410073, P. R. China

[2] Department of Mechanical and Aerospace Engineering, School of Engineering and Applied Science, The George Washington University, 801 22nd St., NW, Washington, DC 20052

Tel.: (202) 994-6149

E-mail: zqkhome@gmail.com, bentzvi@gwu.edu

Received: 29 January 2009 /Accepted: 23 February 2009 /Published: 23 March 2009

Abstract: This paper presents a dynamic model of a rotating beam with a tip mass undergoing large angle, high speed maneuvering. This type of model may also be useful in modeling, analysis and development of various inertial sensors and transducers with similar operating principles. With the consideration of the second-order term of the coupling deformation field, the complete first-order approximated model (CFOAM) of a flexible spacecraft system is developed by using assumed mode method (AMM) and Lagrangian principle. A first-order approximated model (FOAM) is obtained by neglecting the high order terms of the generalized coordinates in CFOAM. A lower order simplified first-order approximated model (SFOAM) is derived by deleting the terms related to the axial deformation. Numerical simulations and theoretical analysis show that: (i) the second-order term has a significant effect on the dynamic characteristics of the system and the dynamic stiffening is accounted for, while the traditional linear approximated model (TLAM) presents invalid simulation results; (ii) the end mass has a 'stiffening' effect on the flexible system in FOAM, but a 'softening' effect in TLAM; and (iii) the SFOAM describes the dynamic behavior well and can be used for controller design. *Copyright © 2009 IFSA.*

Keywords: Flexible structure, Dynamic stiffening, Assumed mode method, Flexible beam

1. Introduction

Rotating flexible beams are used to model light robot arms, elastic linkages, helicopter rotors, satellite solar arrays, and like systems. Modeling and control of systems involving interconnected rigid structures

and flexible appendages is a difficult task to accomplish, as most of these systems generally involve complex dynamics characterized by nonlinearities and strong coupling between flexible and rigid modes. Moreover, modern engineering technology is leading to ever more demanding performance criteria, such as high rotational speeds and large angular maneuvering, increasing precision and pointing accuracy. These criteria have posed serious difficulties for all currently advocated control design methodologies. Proper dynamic modeling of the system is a foundation for further research, such as analysis of the dynamic characteristics and various controller designs.

The hybrid coordinate approach is currently the most widely used method, which describes the deformation field of flexible and rigid bodies separately. Mechanical systems undergoing high–speed rotation can produce dynamic stiffening [1, 2] due to the coupling between rigid motion and elastic deflection, and hence traditional dynamic analysis techniques are hardly applicable. The deformation field, commonly used in structural dynamics, is adopted in order to calculate the kinematics of flexible structures in the system. Therefore, modal characteristic changes due to high rotational speeds are not included in the traditional dynamic model [3].

In most cases, problems arise not because of a lack of available analytical/numerical design procedures, but because of our failure to recognize and appreciate the mechanism of dynamic stiffening. Unlike the research reported in [4,5], where the attempt was to "capture" the dynamic stiffening terms, Hong *et al* [6-8] studied the mechanism of dynamic stiffening, and concluded that the coupling deformation field can explain this phenomenon. Researches [7–10] indicated that the coupling term not included in traditional linear deformation field can have significant effect on the dynamic characteristics of the multibody system when it undergoes large rigid–body motion. The work done by Yang *et al* [7] investigated a hub–beam system by using finite element method, and pointed out that the traditional hybrid coordinate approach may lead to erroneous results in some high–speed systems. In Ref. [9], Kane's methods and the assumed mode method (AMM) were employed to investigate rigid-flexible dynamics of a spacecraft with solar panels. In this paper, we developed the complete first–order approximated model (CFOAM) of a hub–beam system by using the AMM and Lagrangian principle. The corresponding dynamic model of the tip mass is developed in a consistent manner.

This paper is organized as follows. Section 2 describes the flexible hub–beam system and defines the various symbols used. In section 3, the dynamic equations of the flexible system are developed, such as CFOAM, FOAM and SFOAM. In section 4, numerical simulations and comparisons with the traditional linear approximated model (TLAM) are presented to demonstrate the validity of the developed model (CFOAM). Furthermore, the effect of the tip mass on the dynamic characteristics of the hub–beam system is also discussed in the section. The paper concludes with a discussion provided in section 5.

2. System Description

The system shown in Fig. 1 consists of a cantilever beam B built into a rigid body H. The coordinates XY and xy in the figure are defined as the inertial frame and the reference frame, respectively. $\bar{u}_p$ is denoted as the flexible deformation vector at point P with respect to the xy frame, and $\bar{r}_A$ is the radius vector of point A on the hub. θ is considered as rigid body coordinate. After deformation, point P_0 moves to point P.

The beam is characterized by a natural length L, material properties E, ρ, and cross-sectional properties A, I, defined as follows. E and ρ are the modulus of elasticity, and the mass per unit volume of the beam, respectively. The area of the cross section is denoted by A, and the beam area moment of inertia is denoted by I.

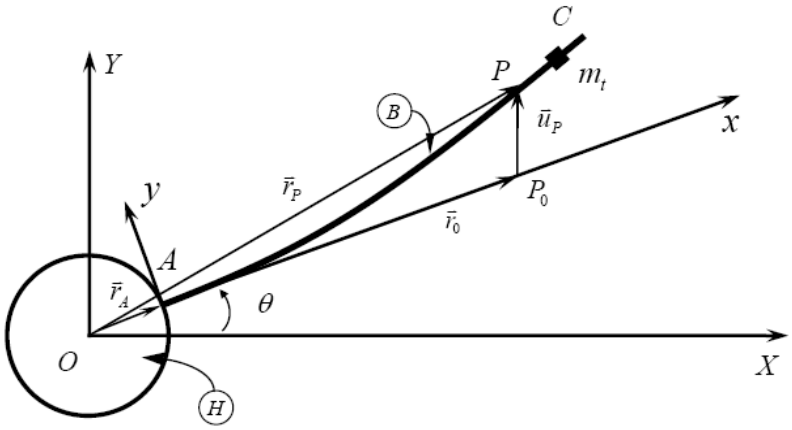

Fig. 1. Beam attached to a moving rigid hub.

3. Equations of Motion

As shown in Fig. 1, the position vector from O to P in the XY frame can be expressed as:

$$\vec{r}_p = \vec{r}_A + \vec{r}_0 + \vec{u}_p, \tag{1}$$

where $\vec{r}_A = \overrightarrow{OA}$, $\vec{r}_0 = \overrightarrow{AP}_0$, and $\vec{u}_p = \overrightarrow{P_0P}$. The coordinates of $\vec{r}_A$ and $\vec{r}_0$ in the OXY frame are represented by $\boldsymbol{r}_A$ and $\boldsymbol{r}_0$, respectively.

As shown in Fig. 2, the coordinate of the deformation vector $\vec{u}_p$ can be represented as:

$$\boldsymbol{u}_p = (u \quad v)^T = (w_1 + w_c \quad w_2)^T, \tag{2}$$

where u and v are the deformation quantities of the point P_0 in the x and y directions in xy frame, respectively; w_1 represents the pure axial deformation, and w_2 represents the transverse deformation along the y–axis. w_c is the deformation associated with the foreshortening quantity due to w_2, and is represented as [7, 8]:

$$w_c = -\frac{1}{2}\int_0^x \left(\frac{\partial w_2}{\partial x}\right)^2 \mathrm{d}x \tag{3}$$

The coordinate of $\vec{r}_p$ in equation (1) may be written in the XY frame as

$$\boldsymbol{r}_p = \boldsymbol{r}_A + \mathbf{Q}(\boldsymbol{r}_0 + \boldsymbol{u}_p) = \mathbf{Q}(r_A\mathbf{e} + \boldsymbol{r}_0 + \boldsymbol{u}_p), \tag{4}$$

where $\boldsymbol{r}_0 = (x \quad 0)^T$, $\boldsymbol{u}_p = (u \quad v)^T$, $\boldsymbol{e} = (1 \quad 0)^T$, and $\boldsymbol{r}_A = r_A(\cos\theta \quad \sin\theta)^T$. As shown in Fig. 2, the variable x is the coordinate of point P_0 in the xy frame, and the parameter $\mathbf{Q}$ is the rotational transformation matrix given by:

$$\mathbf{Q} = \begin{pmatrix} \cos\theta & -\sin\theta \\ \sin\theta & \cos\theta \end{pmatrix}, \tag{5}$$

where θ is the angular displacement of the hub.

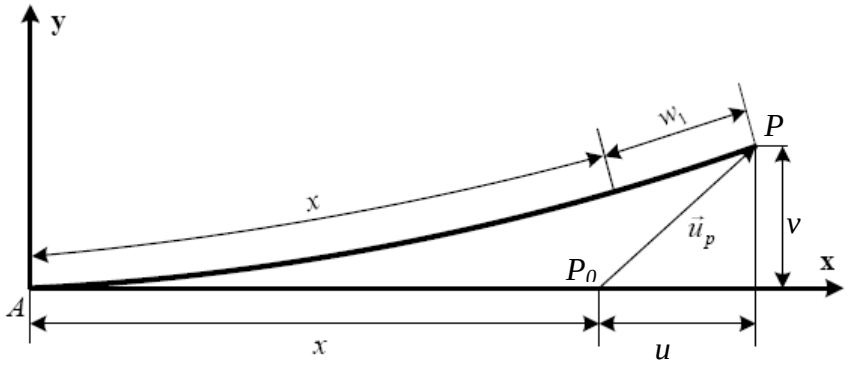

Fig. 2. Description of the beam deformation.

The first-order derivative of $\boldsymbol{r}_P$ may be expressed as

$$\dot{\boldsymbol{r}}_P = \mathbf{QI}(r_A\mathbf{e} + \boldsymbol{r}_0 + \boldsymbol{u}_p)\dot{\theta} + \mathbf{Q}\dot{\boldsymbol{u}}_p \tag{6}$$

where

$$\mathbf{I} = \begin{pmatrix} 0 & -1 \\ 1 & 0 \end{pmatrix}, \qquad \dot{\boldsymbol{u}}_p = \begin{pmatrix} \dot{w}_1 - \dot{w}_c \\ \dot{w}_2 \end{pmatrix}. \tag{7}$$

From Eq. (6), we can derive

$$\dot{\boldsymbol{r}}_P^T\dot{\boldsymbol{r}}_P = \dot{\theta}^2\left\{\left(r_A + w_1 + w_c + x\right)^2 + w_2^2\right\} + \left(\dot{w}_1 + \dot{w}_c\right)^2 + \dot{w}_2^2 + 2\dot{\theta}\left\{\left(r_A + w_1 + w_c + x\right)\dot{w}_2 - \left(\dot{w}_1 + \dot{w}_c\right)v\right\} \tag{8}$$

The kinetic energy of the hub–beam system is written as

$$T = T_h + T_b + T_t = \frac{1}{2}J_h\dot{\theta}^2 + \frac{1}{2}\int_0^L \dot{\boldsymbol{r}}_P^T\dot{\boldsymbol{r}}_P dx + \frac{1}{2}\boldsymbol{m}_t\dot{\boldsymbol{r}}_m^T\dot{\boldsymbol{r}}_m, \tag{9}$$

where T_h, T_b and T_t are the kinetic energy of the hub, beam and tip mass, respectively. J_h is the rotational inertia of the hub. m_t is the weight of the tip mass, r_m is the coordinate of the position vector from O to the tip mass.

By using Euler–Bernoulli theory, the potential energy is given by

$$U = \frac{1}{2}\int_0^L EA\left(\frac{\partial w_1}{\partial x}\right)^2 dx + \frac{1}{2}\int_0^L EI\left(\frac{\partial^2 w_2}{\partial x^2}\right)^2 dx \tag{10}$$

where E is Young's modulus, A is the cross–sectional area and I is the area moment of inertia. The AMM is used to discretize the elastic beam, then the deformations u and v can be represented as:

$$u(x,t) = \sum_{i=1}^{n} f_i^{(1)}(x)q_i^{(1)}(t), \quad v(x,t) = \sum_{i=1}^{n} f_i^{(2)}(x)q_i^{(2)}(t), \tag{11}$$

where $f_i^{(1)}(x)$ and $f_i^{(2)}(x)$ are the admissible functions, $q_i^{(1)}(t)$ and $q_i^{(2)}(t)$ are the mode generalized coordinates, and n refers to the number of included modes. In subsequent derivations, $\boldsymbol{f}_1(x)$, $\boldsymbol{f}_2(x)$, $\boldsymbol{q}_1(t)$ and $\boldsymbol{q}_2(t)$ are adopted to represent the vectors of $f_i^{(1)}(x)$, $f_i^{(2)}(x)$, $q_i^{(1)}(t)$ and $q_i^{(2)}(t)$ respectively. From Eq. (11), Eq. (8) can be rewritten as

$$\begin{aligned}\dot{\boldsymbol{r}}_p^T\dot{\boldsymbol{r}}_p = \dot{\theta}^2\left\{(r_A+x)^2+2(r_A+x)\boldsymbol{f}_1\boldsymbol{q}_1-(r_A+x)\boldsymbol{q}_2^T\boldsymbol{S}\boldsymbol{q}_2+\boldsymbol{q}_1^T\boldsymbol{f}_1^T\boldsymbol{f}_1\boldsymbol{q}_1+\boldsymbol{q}_2^T\boldsymbol{f}_2^T\boldsymbol{f}_2\boldsymbol{q}_2-\boldsymbol{f}_1\boldsymbol{q}_1\boldsymbol{q}_2^T\boldsymbol{S}\boldsymbol{q}_2+\frac{1}{4}\left(\boldsymbol{q}_2^T\boldsymbol{S}\boldsymbol{q}_2\right)^2\right\}\\ +2\dot{\theta}\left\{(r_o+x)\boldsymbol{f}_2\dot{\boldsymbol{q}}_2+\boldsymbol{q}_1^T\boldsymbol{f}_1^T\boldsymbol{f}_2\dot{\boldsymbol{q}}_2-\boldsymbol{q}_2^T\boldsymbol{f}_2^T\boldsymbol{f}_1\dot{\boldsymbol{q}}_1+\boldsymbol{q}_2^T\boldsymbol{S}\dot{\boldsymbol{q}}_2\boldsymbol{f}_2\boldsymbol{q}_2\right\}+\dot{\boldsymbol{q}}_1^T\boldsymbol{f}_1^T\boldsymbol{f}_1\dot{\boldsymbol{q}}_1+\dot{\boldsymbol{q}}_2^T\boldsymbol{f}_2^T\boldsymbol{f}_2\dot{\boldsymbol{q}}_2-2\dot{\boldsymbol{q}}_1^T\boldsymbol{f}_1^T\boldsymbol{q}_2^T\boldsymbol{S}\dot{\boldsymbol{q}}_2+\left(\boldsymbol{q}_2^T\boldsymbol{S}\dot{\boldsymbol{q}}_2\right)^2\end{aligned}, \tag{12}$$

where $\dot{\theta}^2\boldsymbol{f}_1\boldsymbol{q}_1\boldsymbol{q}_2^T\boldsymbol{S}\boldsymbol{q}_2$, $2\dot{\theta}\boldsymbol{q}_2^T\boldsymbol{S}\dot{\boldsymbol{q}}_2\boldsymbol{f}_2\boldsymbol{q}_2$, $2\dot{\boldsymbol{q}}_1^T\boldsymbol{f}_1^T\boldsymbol{q}_2^T\boldsymbol{S}\dot{\boldsymbol{q}}_2$, $\left(\boldsymbol{q}_2^T\boldsymbol{S}\dot{\boldsymbol{q}}_2\right)^2$ and $\frac{1}{4}\dot{\theta}^2\left(\boldsymbol{q}_2^T\boldsymbol{S}\boldsymbol{q}_2\right)^2$ are high order terms related to the generalized coordinates.

3.1. Equations of Motion at the Element Level

To derive the equations of motion in a more compact form, the following element coefficients and matrices are introduced:

$$J_b = \int_0^L \rho A(r_A+x)^2\,dx \tag{13}$$

$$\boldsymbol{K}_1 = \int_0^L EA\left(\frac{\partial \boldsymbol{f}_1(x)}{\partial x}\right)^T\frac{\partial \boldsymbol{f}_1(x)}{\partial x}dx \tag{14}$$

$$\boldsymbol{K}_2 = \int_0^L EI\left(\frac{\partial^2 \boldsymbol{f}_2(x)}{\partial x^2}\right)^T\frac{\partial^2 \boldsymbol{f}_2(x)}{\partial x^2}dx \tag{15}$$

$$\boldsymbol{M}_i = \int_0^L \rho A\boldsymbol{f}_i^T\boldsymbol{f}_i dx, \qquad i=1,2 \tag{16}$$

$$\boldsymbol{V}_i = \int_0^L \rho A(r_A+x)\boldsymbol{f}_i dx \qquad i=1,2 \tag{17}$$

$$\boldsymbol{D} = \int_0^L \rho A(r_A+x)\boldsymbol{S}(x)dx \tag{18}$$

$$\boldsymbol{R} = \int_0^L \rho A\boldsymbol{f}_1^T\boldsymbol{f}_2 dx, \tag{19}$$

where J_b is the rotational inertia of the beam about the hub center, matrices $\boldsymbol{K}_1 \in R^{n\times n}$ and $\boldsymbol{K}_2 \in R^{n\times n}$ are the conventional stiffness matrices, $\boldsymbol{M}_i \in R^{n\times n}, i=1,2$ are generalized elastic mass matrices, matrix $\boldsymbol{D}$ results from the second order term of the coupling deformation field (3), matrix $\boldsymbol{R}$ results from the gyroscopic effects, and $\boldsymbol{S}(x)$ results from w_c and is represented as:

$$\boldsymbol{S}(x) = \int_0^x \frac{\partial \boldsymbol{f}_2^T(\xi)}{\partial \xi}\frac{\partial \boldsymbol{f}_2(\xi)}{\partial \xi}\mathrm{d}\xi \tag{20}$$

It is important to note that matrix $\boldsymbol{D}$ is non-negative definite because $\boldsymbol{S}(x)$ is a non-negative definite matrix.

Using AMM with n assumed modes, Eqs. (9) and (10) can be rewritten as:

$$T = \dot{\theta}^2\left(\frac{1}{2}J_h + \frac{1}{2}J_b + \boldsymbol{V}_1\boldsymbol{q}_1 + \frac{1}{2}\boldsymbol{q}_1^T\boldsymbol{M}_1\boldsymbol{q}_1 + \frac{1}{2}\boldsymbol{q}_2^T\boldsymbol{M}_2\boldsymbol{q}_2 - \frac{1}{2}\boldsymbol{q}_2^T\boldsymbol{D}\boldsymbol{q}_2\right) + \dot{\theta}\left(\boldsymbol{V}_2\dot{\boldsymbol{q}}_2 + \boldsymbol{q}_1^T\boldsymbol{R}\dot{\boldsymbol{q}}_2 - \boldsymbol{q}_2^T\boldsymbol{R}^T\dot{\boldsymbol{q}}_1\right) + \frac{1}{2}\dot{\boldsymbol{q}}_1^T\boldsymbol{M}_1\dot{\boldsymbol{q}}_1$$
$$+\frac{1}{2}\dot{\boldsymbol{q}}_2^T\boldsymbol{M}_2\dot{\boldsymbol{q}}_2 + \int_0^L \rho A\left\{\left(\boldsymbol{q}_2^T\boldsymbol{S}\dot{\boldsymbol{q}}_2\right)^2 - \dot{\theta}^2\boldsymbol{f}_1\boldsymbol{q}_1\boldsymbol{q}_2^T\boldsymbol{S}\boldsymbol{q}_2 + \frac{1}{4}\dot{\theta}^2\left(\boldsymbol{q}_2^T\boldsymbol{S}\boldsymbol{q}_2\right)^2 + 2\dot{\theta}\boldsymbol{q}_2^T\boldsymbol{S}\dot{\boldsymbol{q}}_2\boldsymbol{f}_2\boldsymbol{q}_2 - 2\boldsymbol{f}_1\dot{\boldsymbol{q}}_1\boldsymbol{q}_2^T\boldsymbol{S}\dot{\boldsymbol{q}}_2\right\}dx \tag{21}$$

$$U = \frac{1}{2}\boldsymbol{q}_1^T\boldsymbol{K}_1\boldsymbol{q}_1 + \frac{1}{2}\boldsymbol{q}_2^T\boldsymbol{K}_2\boldsymbol{q}_2 \tag{22}$$

The governing equations of motion can now be obtained through the application of the Lagrangian principle

$$\frac{d}{dt}\left(\frac{\partial T}{\partial \dot{h}_i}\right) - \frac{\partial T}{\partial h_i} + \frac{\partial U}{\partial h_i} = Q_i \qquad i = 1, 2, \cdots, n+1, \tag{23}$$

where η_i are the system generalized coordinates, and Q_i the non-conservative generalized forces due to environmental effects and actuators.

By substituting Eqs. (21) and (22) into Eq.(23), the equations of motion of the flexible system at the element level in compact form can be written as:

$$\begin{bmatrix} M_{\theta\theta} & \boldsymbol{M}_{\theta q_1} & \boldsymbol{M}_{\theta q_2} \\ \boldsymbol{M}_{q_1\theta} & \boldsymbol{M}_{q_1q_1} & \boldsymbol{0} \\ \boldsymbol{M}_{q_2\theta} & \boldsymbol{0} & \boldsymbol{M}_{q_2q_2} \end{bmatrix}\begin{bmatrix} \ddot{\theta} \\ \ddot{\boldsymbol{q}}_1 \\ \ddot{\boldsymbol{q}}_2 \end{bmatrix} + 2\dot{\theta}\begin{bmatrix} 0 & \boldsymbol{0} & \boldsymbol{0} \\ 0 & \boldsymbol{0} & \boldsymbol{G}_{q_1q_2} \\ 0 & \boldsymbol{G}_{q_2q_1} & \boldsymbol{0} \end{bmatrix}\begin{bmatrix} \dot{\theta} \\ \dot{\boldsymbol{q}}_1 \\ \dot{\boldsymbol{q}}_2 \end{bmatrix} + \begin{bmatrix} 0 & \boldsymbol{0} & \boldsymbol{0} \\ 0 & \boldsymbol{K}_{q_1q_1} & \boldsymbol{0} \\ 0 & \boldsymbol{0} & \boldsymbol{K}_{q_2q_2} \end{bmatrix}\begin{bmatrix} \theta \\ \boldsymbol{q}_1 \\ \boldsymbol{q}_2 \end{bmatrix} = \begin{bmatrix} Q_\theta \\ \boldsymbol{Q}_{q_1} \\ \boldsymbol{Q}_{q_2} \end{bmatrix} + \begin{bmatrix} \tau \\ \boldsymbol{0} \\ \boldsymbol{0} \end{bmatrix}, \tag{24}$$

where $\boldsymbol{M}_{\theta\theta} \in R^1$ is the rotary inertia of the system, $\boldsymbol{M}_{q_1q_1} \in R^{n\times n}$ and $\boldsymbol{M}_{q_2q_2} \in R^{n\times n}$ are the beam generalized elastic mass matrices, $\boldsymbol{M}_{\theta q_1} \in R^{1\times n}$, $\boldsymbol{M}_{\theta q_2} \in R^{1\times n}$, $\boldsymbol{M}_{q_1\theta} \in R^{n\times 1}$ and $\boldsymbol{M}_{q_2\theta} \in R^{n\times 1}$ represent the nonlinear inertia coupling between the motion of the reference frame and the elastic deformations, $\boldsymbol{K}_{q_1q_1} \in R^{n\times n}$ and $\boldsymbol{K}_{q_2q_2} \in R^{n\times n}$ are generalized elastic stiffness matrices that are shown to be affected by both the motion of the reference frame and the elastic deformations, Q_θ represents inertia forces, and τ is the rotational external torque. The parameters in Eq. (24) are given as follows:

$$M_{\theta\theta} = J_h + J_b + \boldsymbol{q}_1^T\boldsymbol{M}_1\boldsymbol{q}_1 + \boldsymbol{q}_2^T\boldsymbol{M}_2\boldsymbol{q}_2 + 2\boldsymbol{V}_{11}\boldsymbol{q}_1 - \underline{\boldsymbol{q}_2^T\boldsymbol{D}\boldsymbol{q}_2} + \Delta M_{\theta\theta} \tag{25}$$

$$\boldsymbol{M}_{q_1\theta} = \boldsymbol{M}_{\theta q_1}^T = -\boldsymbol{R}\boldsymbol{q}_2 \tag{26}$$

$$\boldsymbol{M}_{\theta q_2} = \boldsymbol{M}_{q_2\theta}^T = \boldsymbol{V}_{12} + \boldsymbol{q}_1^T\boldsymbol{R} + \Delta\boldsymbol{M}_{q_2\theta}^T \tag{27}$$

$$\boldsymbol{M}_{\theta q_2} = \boldsymbol{M}_{q_2\theta}^T = \boldsymbol{V}_{12} + \boldsymbol{q}_1^T\boldsymbol{R} + \Delta\boldsymbol{M}_{q_2\theta}^T \tag{28}$$

$$\boldsymbol{G}_{q_1q_2} = -\boldsymbol{G}_{q_2q_1}^T = -\boldsymbol{R} \tag{29}$$

$$\boldsymbol{K}_{q_1q_1} = \boldsymbol{K}_1 - \dot{\theta}^2\boldsymbol{M}_1 \tag{30}$$

$$\boldsymbol{K}_{q_2q_2} = \boldsymbol{K}_2 - \dot{\theta}^2\boldsymbol{M}_2 + \underline{\dot{\theta}^2\boldsymbol{D}} \tag{31}$$

$$Q_\theta = -2\dot{\theta}\left[\left(\boldsymbol{q}_1^T\boldsymbol{M}_{1}\dot{\boldsymbol{q}}_1 + \boldsymbol{q}_2^T\boldsymbol{M}_{2}\dot{\boldsymbol{q}}_2\right) + \boldsymbol{V}_1\dot{\boldsymbol{q}}_1 - \underline{\boldsymbol{q}_2^T\boldsymbol{D}\dot{\boldsymbol{q}}_2}\right] + \Delta Q_\theta \tag{32}$$

$$\boldsymbol{Q}_{q_1} = \dot{\theta}^2\boldsymbol{V}_1^T + \Delta\boldsymbol{Q}_{q_1} \tag{33}$$

$$\boldsymbol{Q}_{q_2} = \Delta\boldsymbol{Q}_{q_2}, \tag{34}$$

where

$$\Delta M_{\theta\theta} = \int_0^L \rho A\left\{\frac{1}{2}\left(\boldsymbol{q}_2^T\boldsymbol{S}\boldsymbol{q}_2\right)^2 - 2\boldsymbol{f}_1\boldsymbol{q}_1\boldsymbol{q}_2^T\boldsymbol{S}\boldsymbol{q}_2\right\}dx \tag{35}$$

$$\Delta\boldsymbol{M}_{q_2\theta} = 4\int_0^L \rho A\boldsymbol{f}_2\boldsymbol{q}_2\boldsymbol{S}\boldsymbol{q}_2 dx \tag{36}$$

$$\Delta Q_\theta = 2\int_0^L \rho A\left\{-\boldsymbol{f}_1\dot{\boldsymbol{q}}_1\boldsymbol{q}_2^T\boldsymbol{S}\boldsymbol{q}_2\dot{\theta} + \left(\boldsymbol{q}_2^T\boldsymbol{S}\boldsymbol{q}_2\right)\left(\boldsymbol{q}_2^T\boldsymbol{S}\dot{\boldsymbol{q}}_2\right)\dot{\theta} - 2\boldsymbol{f}_1\boldsymbol{q}_1\boldsymbol{q}_2^T\boldsymbol{S}\dot{\boldsymbol{q}}_2\dot{\theta} + \dot{\boldsymbol{q}}_2^T\boldsymbol{S}\dot{\boldsymbol{q}}_2\boldsymbol{f}_2\boldsymbol{q}_2 + \boldsymbol{q}_2^T\boldsymbol{S}\ddot{\boldsymbol{q}}_2\boldsymbol{f}_2\boldsymbol{q}_2 + \boldsymbol{q}_2^T\boldsymbol{S}\dot{\boldsymbol{q}}_2\boldsymbol{f}_2\dot{\boldsymbol{q}}_2\right\}dx \tag{37}$$

$$\Delta\boldsymbol{Q}_{q_1} = -\int_0^L \rho A\left\{2\boldsymbol{f}_1^T\dot{\boldsymbol{q}}_2^T\boldsymbol{S}\dot{\boldsymbol{q}}_2 + 2\boldsymbol{f}_1^T\boldsymbol{q}_2^T\boldsymbol{S}\ddot{\boldsymbol{q}}_2 + \dot{\theta}^2\boldsymbol{f}_1^T\boldsymbol{q}_2^T\boldsymbol{S}\boldsymbol{q}_2\right\}dx \tag{38}$$

$$\begin{aligned}\Delta\boldsymbol{Q}_{q_2} = \int_0^L \rho A\Big\{&2\dot{\theta}\boldsymbol{f}_2\dot{\boldsymbol{q}}_2\boldsymbol{S}\boldsymbol{q}_2 + 2\dot{\theta}\boldsymbol{f}_2\boldsymbol{q}_2\boldsymbol{S}\dot{\boldsymbol{q}}_2 - 2\boldsymbol{f}_1\ddot{\boldsymbol{q}}_1\boldsymbol{S}\boldsymbol{q}_2 - 2\boldsymbol{f}_1\dot{\boldsymbol{q}}_1\boldsymbol{S}\dot{\boldsymbol{q}}_2 + 2\dot{\boldsymbol{q}}_2^T\boldsymbol{S}\dot{\boldsymbol{q}}_2\boldsymbol{S}\boldsymbol{q}_2 + 2\dot{\theta}\boldsymbol{q}_2^T\boldsymbol{S}\dot{\boldsymbol{q}}_2\boldsymbol{f}_2^T + 2\dot{\theta}\boldsymbol{f}_2\boldsymbol{q}_2\boldsymbol{S}\dot{\boldsymbol{q}}_2\\ &+ 2\boldsymbol{q}_2^T\boldsymbol{S}\ddot{\boldsymbol{q}}_2\boldsymbol{S}\boldsymbol{q}_2 + 2\boldsymbol{q}_2^T\boldsymbol{S}\dot{\boldsymbol{q}}_2\boldsymbol{S}\dot{\boldsymbol{q}}_2 - 2\boldsymbol{f}_1\boldsymbol{q}_1\boldsymbol{S}\boldsymbol{q}_2\dot{\theta}^2 + \boldsymbol{q}_2^T\boldsymbol{S}\boldsymbol{q}_2\boldsymbol{S}\boldsymbol{q}_2\dot{\theta}^2 - 2\boldsymbol{f}_1\dot{\boldsymbol{q}}_1\boldsymbol{S}\dot{\boldsymbol{q}}_2 + 2\left(\boldsymbol{q}_2^T\boldsymbol{S}\dot{\boldsymbol{q}}_2\right)\boldsymbol{S}\dot{\boldsymbol{q}}_2\Big\}dx\end{aligned} \tag{39}$$

Equations (35)-(39) are derived from the high order terms in Eq. (12).

In Eq. (24), the nonlinear coupling between the rigid–body motion and the elastic deformations can be easily seen. The underlined terms in Eqs. (25), (31) and (32) result from the coupling deformation field. The newly established Eqs. (24)-(34) are called the complete first-order approximate model(CFOAM), while the CFOAM without Eqs.(35)-(39) are called the first-order approximate model (FOAM). The FOAM without the underlined terms are called traditional linear approximate model (TLAM). A simplified first-order approximate model (SFOAM) of the hub-beam system can be derived from FOAM by deleting the elements related to Q_θ, $\boldsymbol{q}_1$ and $\dot{\boldsymbol{q}}_1$:

$$\begin{bmatrix} M_{\theta\theta} & \boldsymbol{M}_{\theta q_2} \\ \boldsymbol{M}_{q_2\theta} & \boldsymbol{M}_{q_2q_2}\end{bmatrix}\begin{bmatrix}\ddot{\theta}\\ \ddot{\boldsymbol{q}}_2\end{bmatrix} + \begin{bmatrix}0 & \boldsymbol{0}\\ \boldsymbol{0} & \boldsymbol{K}_{q_2q_2}\end{bmatrix}\begin{bmatrix}\theta\\ \boldsymbol{q}_2\end{bmatrix} = \begin{bmatrix}\tau\\ \boldsymbol{0}\end{bmatrix}, \tag{40}$$

where $M_{\theta\theta}$, $\boldsymbol{M}_{\theta q_2}$, $\boldsymbol{M}_{q_2\theta}$, $\boldsymbol{M}_{q_2q_2}$ and $\boldsymbol{K}_{q_2q_2}$ can also be obtained by deleting the elements related to $\boldsymbol{q}_1$ and $\dot{\boldsymbol{q}}_1$ in (25), (27), (28), (31) and(32). It is noted that SFOAM can be used for controller design.

3.2. Tip Mass Dynamics

The tip mass, as shown in Fig. 1, is located at a distance l along the undeformed beam from point A. It is considered to have a mass m_t. The position vector of the tip mass with respect to the inertial frame XY can be represented as

$$\boldsymbol{r}_m = \boldsymbol{r}_A + \mathbf{Q}(\boldsymbol{r}_t + \boldsymbol{u}_t), \tag{41}$$

where $\boldsymbol{r}_t = (l \quad 0)^T$ is the position vector of the tip mass in the reference frame xy in the undeformed configuration, and $\boldsymbol{u}_t$ is the elastic displacement vector of the point on the beam to which the tip mass is attached.

The contribution of the tip mass to FOAM of the multibody system can also be included by applying the Lagrangian principle. The equations can be represented by the following matrix form:

$$\begin{bmatrix} M^l_{\theta\theta} & \boldsymbol{M}^{\ l}_{\theta q_1} & \boldsymbol{M}^{\ l}_{\theta q_2} \\ \boldsymbol{M}^{\ l}_{q_1\theta} & \boldsymbol{M}^{\ l}_{q_1 q_1} & \boldsymbol{0} \\ \boldsymbol{M}^{\ l}_{q_2\theta} & \boldsymbol{0} & \boldsymbol{M}^{\ l}_{q_2 q_2} \end{bmatrix} \begin{bmatrix} \ddot{\theta} \\ \ddot{\boldsymbol{q}}_1 \\ \ddot{\boldsymbol{q}}_2 \end{bmatrix} + 2\dot{\theta} \begin{bmatrix} 0 & \boldsymbol{0} & \boldsymbol{0} \\ \boldsymbol{0} & \boldsymbol{0} & \boldsymbol{G}^{\ l}_{q_1 q_2} \\ \boldsymbol{0} & \boldsymbol{G}^{\ l}_{q_2 q_1} & \boldsymbol{0} \end{bmatrix} \begin{bmatrix} \dot{\theta} \\ \dot{\boldsymbol{q}}_1 \\ \dot{\boldsymbol{q}}_2 \end{bmatrix} + \begin{bmatrix} 0 & \boldsymbol{0} & \boldsymbol{0} \\ \boldsymbol{0} & \boldsymbol{K}^{\ l}_{q_1 q_1} & \boldsymbol{0} \\ \boldsymbol{0} & \boldsymbol{0} & \boldsymbol{K}^{\ l}_{q_2 q_2} \end{bmatrix} \begin{bmatrix} \theta \\ \boldsymbol{q}_1 \\ \boldsymbol{q}_2 \end{bmatrix} = \begin{bmatrix} Q^l_{\theta} \\ \boldsymbol{Q}^{\ l}_{q_1} \\ \boldsymbol{0} \end{bmatrix}, \tag{42}$$

where the coefficients and matrices are shown in the appendix.

3.3. Equations of Motion of the Whole System

The FOAM of the whole system can be obtained from Eqs. (24) and (42) directly by adding the corresponding entries of the generalized matrices. Two different models are developed in order to examine the effect of the second order term. The established equations with and without the underlined terms are called FOAM and TLAM, respectively.

4. Simulations and Results

The physical parameters of the flexible hub-beam system are shown in Table 1. The payload is represented by a point mass m_t at the free end of the beam. The number of included modes n is 5.

Table 1. Physical parameters.

Property	Symbol	Value
Beam length	L	8m
Mass per unit volume	ρ	2.7667×103 kg/m^3
Cross-Section	A	7.2968×10-5 m^2
Young's modulus	E	6.8952×1010 N/m^2
Beam area moment of inertia	I	8.2189×10-9m^4
Hub moment of inertia	J_h	200 kgm^2
Hub radius	r	0.5 m
Tip mass	m_t	0.1 kg

The response of the flexible motion is simulated by assuming that the slewing motion follows a prescribed trajectory, and the maneuver profile [2] is given by

$$\dot{\theta} = \begin{cases} \dfrac{w_f}{t_f} - \dfrac{w_f}{2\pi} \sin\left(\dfrac{2\pi}{t_f} t\right), & 0 \le t \le t_f \\ w_f, & t > t_f \end{cases} \tag{43}$$

where w_f and t_f represent the velocity of the hub at the end of the maneuver, and the time to reach the maximum velocity, respectively.

4.1. Vibration Response of CFOAM and FOAM

Let us consider first CFOAM and FOAM of the hub–beam system without a tip mass.

The terms (35)-(39) in CFOAM are the integrations of the generalized coordinates. Thus, CFOAM is not only complicated in presentation, but also difficult in symbolic computation and numerical simulation. Fig. 3 shows the simulation results with the neglected terms when w_f is 3 rad/s. For simplicity, the first mode is taken into account. In fact, it dominates the transverse response of the beam (see Fig. 6). We can see from Fig. 3 that these terms have small amplitude and tend to reach zero after 30 s.

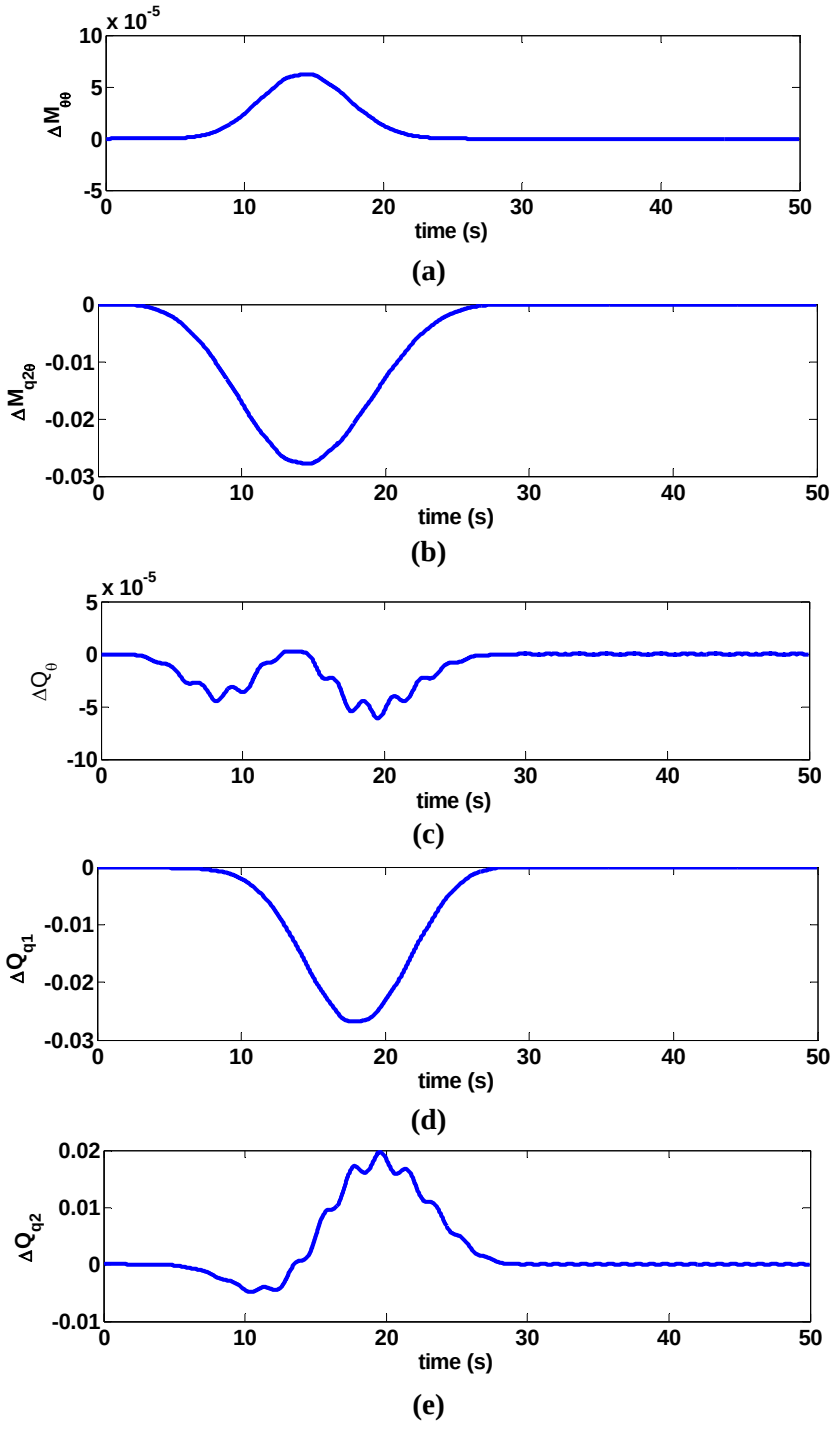

Fig. 3. Response with the neglected terms when w_f =3 rad/s.

Fig. 4 shows that the displacement of CFOAM and FOAM is exactly the same. This confirms that the simplification is valid and FOAM can be used to investigate the dynamic characteristics of the flexible multibody system.

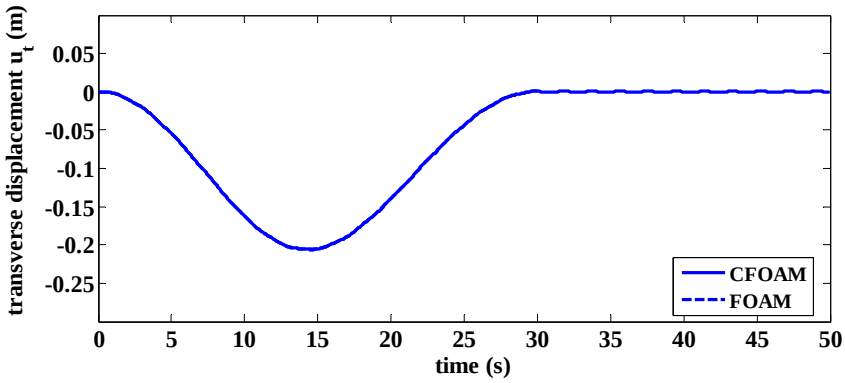

Fig. 4. Tip displacement of CFOAM and FOAM when w_f =3 rad/s.

4.2. Vibration Response of FOAM and TLAM

Fig. 5 shows the simulation results of TLAM and FOAM for comparison. It can be seen that the vibration response of the flexible beam diverges when the angular velocity is greater than 3rad/s. It should be noted that the resulting tip displacement of TLAM has exceeded the assumption of small deformations. When the angular velocity is smaller than 3rad/s but close to the critical value, e.g., 2.8rad/s, the maximum tip deflection of TLAM is much larger than that of FOAM, which are approximately 0.49m and 0.22m, respectively. Moreover, the residual vibration amplitude of TLAM is approximately 100 times larger than that of FOAM. It can be concluded therefore that TLAM is invalid for describing the deformation of multibody systems in high–speed cases.

Because the second order term in the deformation is not included, the generalized elastic stiffness matrix in the TLAM is expressed as $\boldsymbol{K}_{q_2q_2} = \boldsymbol{K}_2 - \dot{\theta}^2 \boldsymbol{M}_2$. From this expression, it is seen that the stiffness matrix may be negative definite when the angular velocity surpasses a critical value. In fact, it can be calculated from Eq. (31) that the critical angular velocity is 2.91rad/s. This is the first order natural circle frequency of the beam according to Table 2. The frequencies evaluated with TLAM are 'softening' compared to the natural frequencies. On the other hand, the generalized elastic stiffness matrix in FOAM is expressed as $\boldsymbol{K}_{q_2q_2} = \boldsymbol{K}_2 - \dot{\theta}^2 \boldsymbol{M}_2 + \underline{\dot{\theta}^2 \boldsymbol{D}}$, in which the underlined term $\dot{\theta}^2 \boldsymbol{D}$ is non–negative definite, and can make $\boldsymbol{K}_{q_2q_2}$ definite positive.

As shown in Table 2, the natural vibration frequency is larger than that evaluated with TLAM, but less than that evaluated with FOAM, i.e. the second order term in coupling deformation field has a 'stiffening' effect on the frequencies of the multibody system in high-speed case. The difference values become larger when the speed increases.

Table 2. The inertia force under different torques.

Mode order	1	2	3	4	5
Natural frequency	0.4635	2.9047	8.1332	15.9377	26.3462
TLAM (1 rad/s)	0.4353	2.9003	8.1316	15.9369	26.3457
FOAM (1 rad/s)	0.4714	2.9308	8.1618	15.9682	26.3776

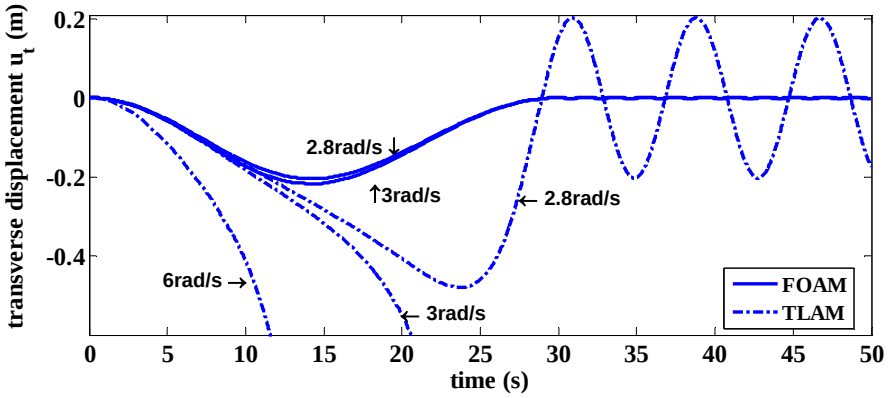

(a) Transverse response of the tip of the beam.

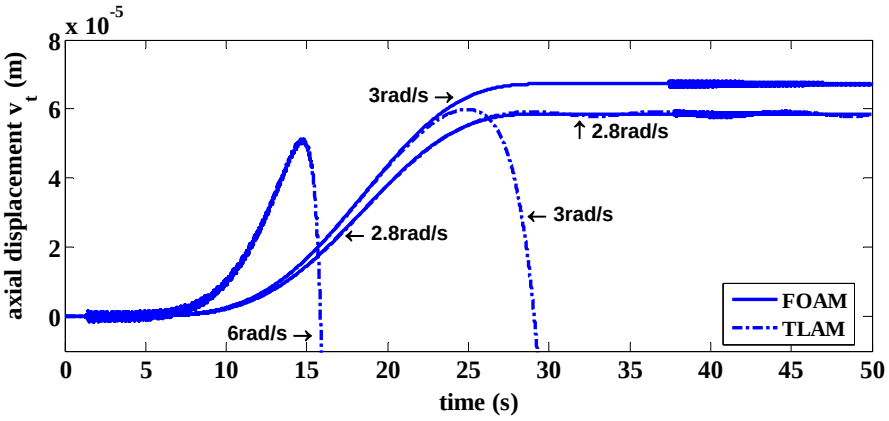

(b) Axial response of the tip of the beam.

Fig. 5. Beam vibration response with respect to different angular velocities.

4.3. Vibration Response of FOAM and SFOAM

Consider first FOAM of the hub–beam system without tip mass. For $w_f = 5rad/s$, and $t_f = 30s$, the resulting response of the first five modes of the flexible hub–beam system is shown in Fig. 6.

It can be seen that the peak response of the transverse displacement is approximately 1500 times larger than that of the axial displacement. As shown in Fig. 6a, the response of the first two modes dominates over the response of the higher modes. Thus the elements related to $\boldsymbol{q}_1$ and $\dot{\boldsymbol{q}}_1$ in (25) can be neglected for simplification. Fig. 6b clearly shows that the simulation results for the different number of modes are exactly the same.

Next, we assume that the torque acting on the rigid hub has the following profile:

$$\tau(t) = \begin{cases} \tau_m \sin\left(\dfrac{2\pi}{T}t\right), & 0 \le t \le t_f \\ 0, & t > t_f \end{cases}, \tag{44}$$

where $t_f = 10s$ is the maneuver time, and τ_m is the maximum torque.

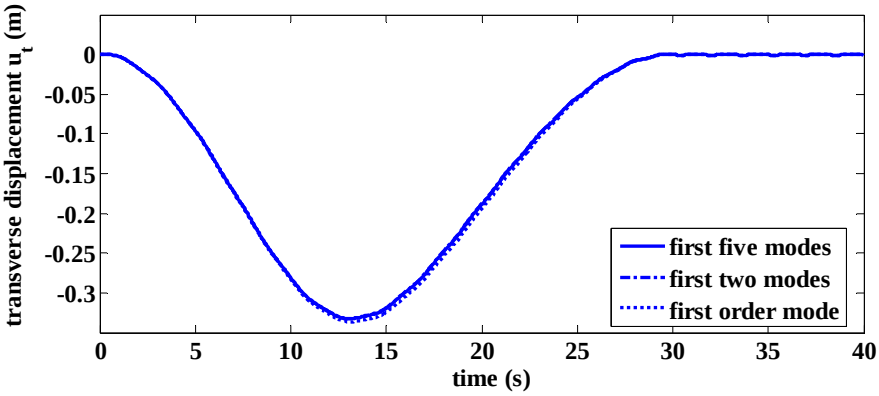

(a) Response of the transverse displacement.

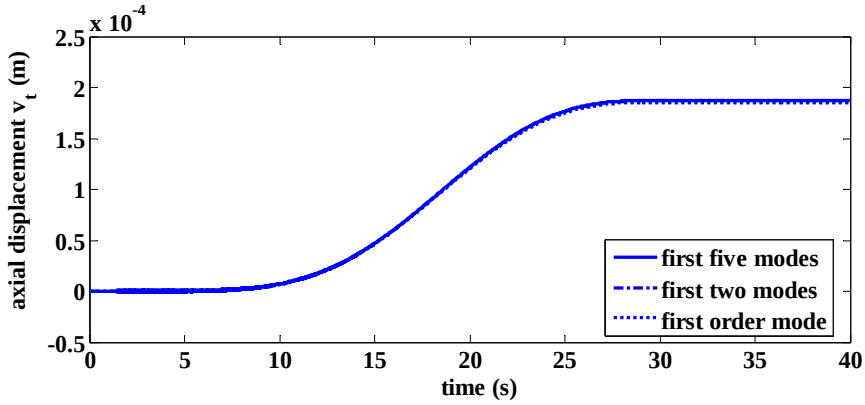

(b) Response of the axial displacement.

Fig. 6. Beam vibration response to prescribed slew maneuver.

As shown in Fig. 7, the maximum amplitude of Q_θ is 2.62 Nm, which is about 6.5 % of τ_m. Table 3 outlines the maximum amplitudes of the generated Q_θ with different $\tau(t)$ acting on the hub. It is clear that Q_θ is small and hence can be treated as a small disturbance of $\tau(t)$. Therefore, for simplification, it is not included in SFOAM.

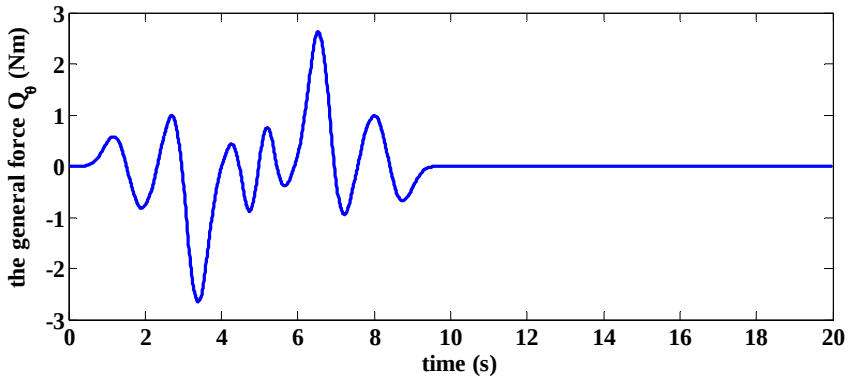

Fig. 7. Response of Q_θ when τ_m is 400Nm.

Table 3. The first five vibration frequencies (Hz).

Torque	**Value (Nm)**			
τ_m	50.0	100	200	400
Q_θ	6.24×10^{-3}	4.61×10^{-2}	3.72×10^{-2}	2.62

Fig. 8 shows the simulation results of FADM and SFOAM. When the torque is small (50 Nm), as shown in Fig. 8 a, the simulation curves of SFADM almost coincided with that of FOAM. But the difference appears when τ_m is 200 Nm. Fig. 8 b shows that the phase of the residual vibration of SFOAM is leading that of FOAM by 0.45 rad, but the amplitude is 24% smaller than that of the latter. We can also see that the displacement of SFOAM is exactly the same (see Fig. 8 b). That is, SFOAM with the first mode reflects the dynamic characteristic of the hub-beam system well, and can be used for controller design.

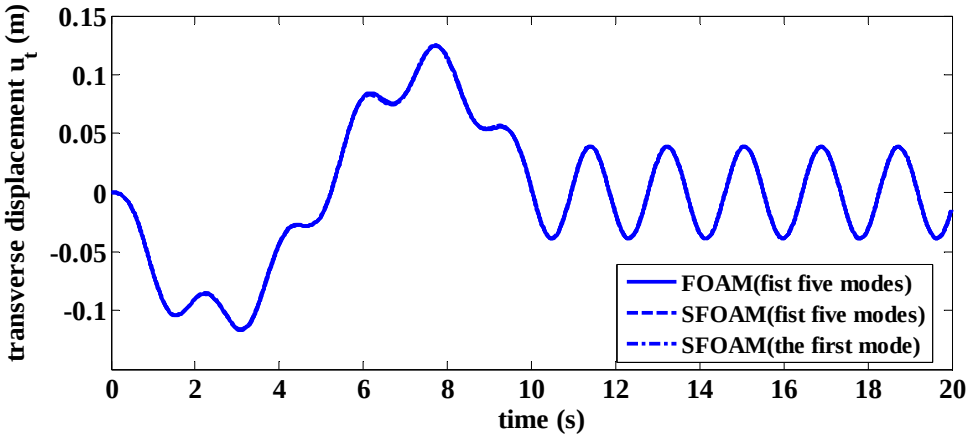

(a) τ_m is 50Nm.

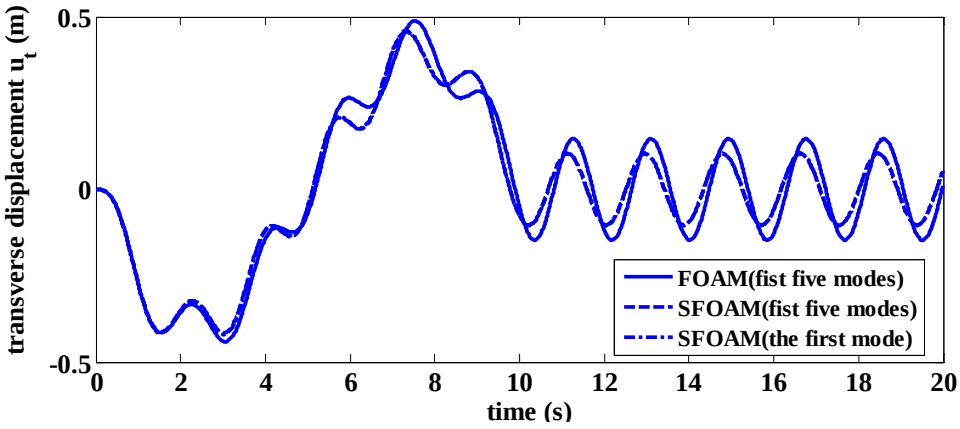

(b) τ_m is 200Nm.

Fig. 8. Tip displacement of the beam when τ_m are 50Nm and 200Nm.

4.4. Vibration Response of Hub-beam System with Tip Mass

The general elastic stiffness matrix of the whole system in TLAM is $\boldsymbol{K}_{22} = \boldsymbol{K}_2 - \dot{\theta}^2 \boldsymbol{M}_2 - m_t \boldsymbol{f}_2^T(l)\boldsymbol{f}_2(l)\dot{\theta}^2$, which shows that the positive definite property of the stiffness matrix in TLAM is determined by the

position r_t, the angular velocity $\dot{\theta}$ and the mass m_t. It is known that the positive definite property of $\boldsymbol{K}_{22}$ is determined by the sign of its eigenvalues. Fig. 9 shows this relationship.

As shown in the figure, the critical velocity is 2.91 rad/s when m_t is located on the hub ($l = 0$). If the angular velocity exceeds the critical value, the dominant eigenvalues of $\boldsymbol{K}_{22}$ will be negative , which can explain the simulation results shown in Fig. 4 (with 3 rad/s). When the tip mass is located at the tip of the beam, the critical velocities are 2.60 rad/s and 1.91 rad/s for m_t=*0.1 kg* and m_t=*0.5 kg*, respectively. Fig. 10 shows the transverse displacement of TLAM for the above two cases. For m_t=*0.5 kg*, TLAM fails to describe the deformation of the flexible beam when the angular velocity is 2.0 rad/s. However, for the same angular velocity, the simulation result of TLAM is almost the same as for FOAM when m_t=*0*. It is seen that the tip mass decreases the critical angular velocity. Moreover, it can be concluded that as the weight increases, the critical value decreases.

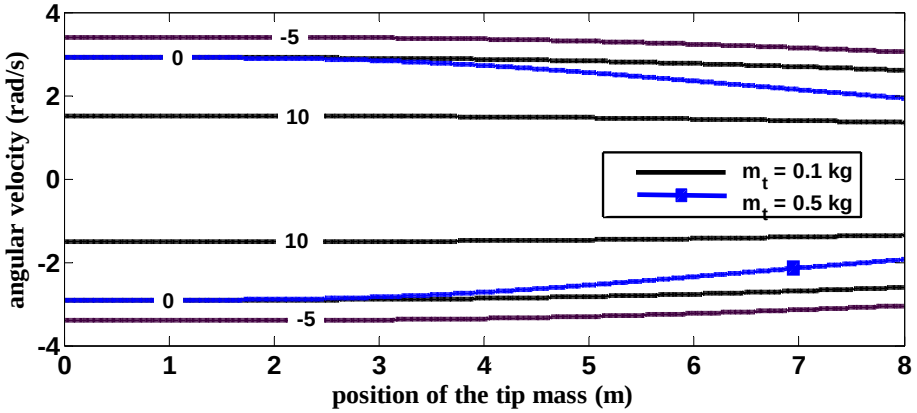

Fig. 9. The dominant eigenvalues of $\boldsymbol{K}_{22}$.

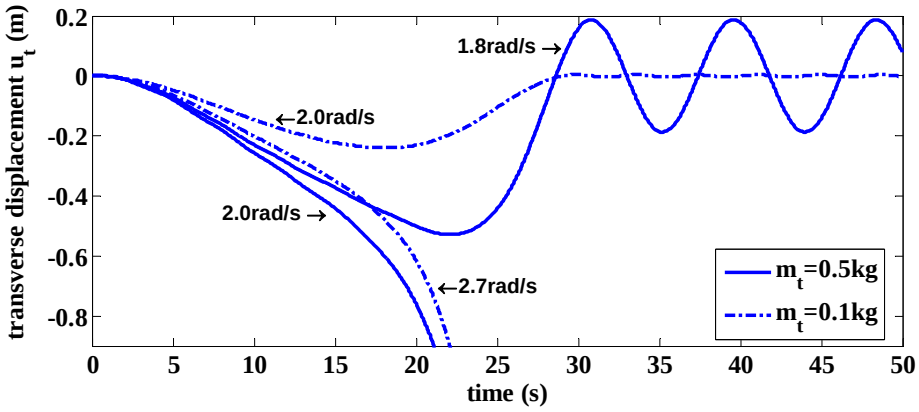

Fig. 10. Response of TLAM system with tip mass.

The generalized elastic stiffness matrix of the tip mass is expressed as $\boldsymbol{K}^{l}_{q_2 q_2} = -m_t \boldsymbol{f}_2^{T}(l)\boldsymbol{f}_2(l)\dot{\theta}^2$, which has a 'softening' effect on the flexible hub–beam system. Because the second order term in coupling deformation is included, the generalized elastic stiffness matrix in FOAM has the term $m_t\left(r_A + L\right)\dot{\theta}^2\boldsymbol{S}$, which acts as a 'stiffening' effect.

5. Conclusions

In this paper, the CFOAM, FOAM and SFOAM of a flexible hub–beam system with a tip mass have been presented by using AMM and Lagrangian principle. It is shown that the traditional hybrid co-ordinate approach cannot account for dynamic stiffening and may lead to erroneous results in some high-speed systems. In contrast, the models we developed in this paper can predict valid results. It was also shown that SFOAM model can be used for controller design. The tip mass has a 'softening' effect on the hub-beam system in TLAM, but has a 'stiffening' effect in FOAM. Theoretical analysis and simulation results show that FOAM has better adaptability than TLAM, especially in cases with high rotational speeds. As a future research, experimental investigations on such a system are needed.

Appendix

The coefficients and matrices in the equation of motion of the tip mass are given as follows:

$$M^{l}_{\theta\theta} = m_t\left(r_A + l\right)^2 + m_t \boldsymbol{q}_1^T \boldsymbol{f}_1^T(l)\boldsymbol{f}_1(l)\boldsymbol{q}_1 + m_t \boldsymbol{q}_2^T \boldsymbol{f}_2^T(l)\boldsymbol{f}_2(l)\boldsymbol{q}_2 + 2m_t\left(r_A + L\right)\boldsymbol{f}_1(l)\boldsymbol{q}_1 - m_t\left(r_A + L\right)\boldsymbol{q}_2^T \boldsymbol{S}\boldsymbol{q}_2 \tag{A1}$$

$$\boldsymbol{M}^{l}_{q_1\theta} = \left(\boldsymbol{M}^{l}_{\theta q_1}\right)^T = -m_t \boldsymbol{f}_1^T(l)\boldsymbol{f}_2(l)\boldsymbol{q}_2 \tag{A2}$$

$$\boldsymbol{M}^{l}_{\theta q_2} = \left(\boldsymbol{M}^{l}_{q_2\theta}\right)^T = m_t\left(r_A + L\right)\boldsymbol{f}_2(l) + \boldsymbol{q}_1^T m_t \boldsymbol{f}_1^T(l)\boldsymbol{f}_2(l) \tag{A3}$$

$$\boldsymbol{M}^{l}_{q_1 q_1} = m_t \boldsymbol{f}_1^T(l)\boldsymbol{f}_1(l) \tag{A4}$$

$$\boldsymbol{M}^{l}_{q_2 q_2} = m_t \boldsymbol{f}_2^T(l)\boldsymbol{f}_2(l) \tag{A5}$$

$$\boldsymbol{G}^{l}_{q_1 q_2} = -\left(\boldsymbol{G}^{l}_{q_2 q_1}\right)^T = -m_t \boldsymbol{f}_1^T(l)\boldsymbol{f}_2(l) \tag{A6}$$

$$\boldsymbol{K}^{l}_{q_1 q_1} = -m_t \boldsymbol{f}_1^T(l)\boldsymbol{f}_1(l)\dot{\theta}^2 \tag{A7}$$

$$\boldsymbol{K}^{l}_{q_2 q_2} = -m_t \boldsymbol{f}_2^T(l)\boldsymbol{f}_2(l)\dot{\theta}^2 + m_t\left(r_A + L\right)\dot{\theta}^2 \boldsymbol{S} \tag{A8}$$

$$\boldsymbol{Q}^{l}_{\theta} = -\dot{\theta}\left[m_t \boldsymbol{q}_1^T \boldsymbol{f}_1^T(l)\boldsymbol{f}_1(l)\dot{\boldsymbol{q}}_1 + m_t \boldsymbol{q}_2^T \boldsymbol{f}_2^T(l)\boldsymbol{f}_2(l)\dot{\boldsymbol{q}}_2 + m_t\left(r_A + L\right)\boldsymbol{f}_1(l)\dot{\boldsymbol{q}}_1 - m_t\left(r_A + L\right)\boldsymbol{q}_2^T \boldsymbol{S}\dot{\boldsymbol{q}}_2\right] \tag{A9}$$

$$\boldsymbol{Q}^{l}_{q_1} = m_t\left(r_A + L\right)\dot{\theta}^2 \boldsymbol{f}_1^T(l) \tag{A10}$$

References

[1]. T. R. Kane, R. R. Ryan, and A. K. Banerjee, Dynamics of a cantilever beam attached to a moving base, *Journal of Guidance, Control, and Dynamics*, Vol. 10, Issue 2, 1987, pp. 139-150.

[2]. R. Jeha, K. Sung-Sup, and K. Sung-Soo, A general approach to stress stiffening effects on flexible multibody dynamic systems, *Mechanics of Structures and Machines*, Vol. 22, Issue 2, 1994, pp. 157-180.

[3]. P. Shi, J. Mcphee, and G. R. Heppler, A deformation field for Euler-Bernoulli beams with applications to flexible multibody dynamics, *Multibody System Dynamics*, Issue 5, 2001, pp. 79-104.

[4]. A. K. Banerjee and J. M. Dickens, Dynamics of an arbitrary flexible body in large rotation and translation, *Journal of Guidance, Control, and Dynamics*, Vol. 13, Issue 2, 1990, pp. 221-227.

[5]. J. Mayo and J. Dominguez, Geometrically nonlinear formulation of flexible multibody systems in terms of beam elements: geometric stiffness, *Computers and Structures*, Vol. 59, 1996, pp. 1039-1050.
[6]. J. Hong and C. You, Advances in dynamics of rigid-flexible coupling system, *Journal of Dynamics and Control*, Vol. 2, Issue 2, 2004, pp. 1-6, (in Chinese).
[7]. H. Yang, J. Hong, and Z. Yu, Dynamics modeling of a flexible hub-beam system with a tip mass, *Journal of Sound and Vibration*, Vol. 266, Issue 4, 2003, pp. 759-774.
[8]. J. Liu and J. Hong, Geometric stiffening of flexible link system with large overall motion, Computers and Structures, Vol. 81, 2003, pp. 2829-2841.
[9]. J. Jang and D. Li, Research on rigid-flexible coupling dynamics of spacecraft with solar panel, *Acta Aeronautica et Astronautica Sinica*, Vol. 27, Issue 3, 2006, pp. 418-422 (in Chinese).
[10]. D. Zhang and Z. Zhu, Dynamic stiffening of rigid-flexible coupling system, *Journal of Nanjing University of Science and Technology*, Vol. 30, Issue 1, 2006, pp. 21-25.

2009 Copyright ©, International Frequency Sensor Association (IFSA). All rights reserved.
(http://www.sensorsportal.com)

IRF'2009

INTEGRITY - RELIABILITY - FAILURE

CHALLENGES AND OPPORTUNITIES

Third International Conference

Faculty of Engineering, University of Porto

Porto-Portugal, July 20-24, 2009

TOPICS OF INTEREST

The conference will address the following main topics:

Analytical and Numerical Tools
Instrumentation and Measurement
Testing and Diagnostics
Nanotechnologies and Nanomaterials
Surface and Interface Engineering
Modes of Failure
Design Against Failure
Energy and Environment

SUMMARY OF DEADLINES

Receipt of Abstracts	28 February, 2009
Acceptance Letters	21 March, 2009
Deadline for Early Registration	31 March, 2009
Receipt of Full Papers for CD	10 May, 2009

INTERNET ACCESS

All conference information, including titles, registration, hotels, social program, sessions and papers schedule is provided at the conference webpage:
http://paginas.fe.up.pt/clme/IRF2009/index.htm

For additional information, please contact either of the Conference Chairs:

Prof. J.F. Silva Gomes
Departamento de Engenharia Mecânica e Gestão Industrial
Faculdade de Engenharia da Universidade do Porto
Rua Dr. Roberto Frias, 4200-465 Porto, Portugal
Tel: (351)-91 725 8950; Fax:(351)-22 508 1771
E-mail: sg@fe.up.pt

Prof. Shaker A. Meguid
Department of Mechanical and Industrial Engineering
University of Toronto
5, King's College, Toronto ON, M5S 3G8, Canada
Tel: (1)-416 978 5741; Fax: (1)-416 978 7753
E-mail: meguid@mie.utoronto.ca

Sensors & Transducers Journal

Guide for Contributors

Aims and Scope

Sensors & Transducers Journal (ISSN 1726-5479) provides an advanced forum for the science and technology of physical, chemical sensors and biosensors. It publishes state-of-the-art reviews, regular research and application specific papers, short notes, letters to Editor and sensors related books reviews as well as academic, practical and commercial information of interest to its readership. Because it is an open access, peer review international journal, papers rapidly published in *Sensors & Transducers Journal* will receive a very high publicity. The journal is published monthly as twelve issues per annual by International Frequency Association (IFSA). In additional, some special sponsored and conference issues published annually.

Topics Covered

Contributions are invited on all aspects of research, development and application of the science and technology of sensors, transducers and sensor instrumentations. Topics include, but are not restricted to:

- Physical, chemical and biosensors;
- Digital, frequency, period, duty-cycle, time interval, PWM, pulse number output sensors and transducers;
- Theory, principles, effects, design, standardization and modeling;
- Smart sensors and systems;
- Sensor instrumentation;
- Virtual instruments;
- Sensors interfaces, buses and networks;
- Signal processing;
- Frequency (period, duty-cycle)-to-digital converters, ADC;
- Technologies and materials;
- Nanosensors;
- Microsystems;
- Applications.

Submission of papers

Articles should be written in English. Authors are invited to submit by e-mail editor@sensorsportal.com 6-14 pages article (including abstract, illustrations (color or grayscale), photos and references) in both: MS Word (doc) and Acrobat (pdf) formats. Detailed preparation instructions, paper example and template of manuscript are available from the journal's webpage: http://www.sensorsportal.com/HTML/DIGEST/Submition.htm Authors must follow the instructions strictly when submitting their manuscripts.

Advertising Information

Advertising orders and enquires may be sent to sales@sensorsportal.com Please download also our media kit: http://www.sensorsportal.com/DOWNLOADS/Media_Kit_2008.pdf

IFSA
www.sensorsportal.com

e-Impact Factor 2008:
205.767

Subscription 2009

Sensors & Transducers Journal (ISSN 1726-5479) for scientists and engineers who need to be at cutting-edge of sensor and measuring technologies and their applications.

Keep up-to-date with the latest, most significant advances in all areas of sensors and transducers.

Take an advantage of IFSA membership and save 40 % of subscription cost.

Subscribe online:
http://www.sensorsportal.com/HTML/DIGEST/Journal_Subscription_2009.htm
e-mail: editor@sensorsportal.com
tel. +34 696 06 77 16

www.sensorsportal.com